EXPERIMENTAL STUDY OF A LAMINAR PREMIXED LFG/AIR FLAME IN A SLOT BURNER USING MACH-ZEHNDER INTERFEROMETRY

by

Zabihollah NAJAFIAN ASHRAFI[a]* and Mehdi ASHJAEE[a]

[a] School of Mechanical Engineering, University of Tehran, Tehran, Iran

Original scientific paper
DOI:10.2298/TSCI141113147N

An experimental study was conducted to investigate the influence of Reynolds number and equivalence ratio on flame temperature field and thermal flame height of laminar premixed landfill gas fuel. Mach-Zehnder interferometry technique is used to obtain an insight to the overall temperature field. The slot burner with large aspect ratio, length of 60 mm and width of 6 mm, was used to eliminate the three-dimensional effect of temperature field. Two kinds of mixed fuels, LFG_{70} (70% CH_4-30% CO_2 on volume basis) and LFG_{50} (50% CH_4-50% CO_2) were used to investigate flame characteristics under the test conditions of $100 \leq Re \leq 600$ and $0.7 \leq \varphi \leq 1.3$. The present measurement reveals that the variation of maximum flame temperature with increment of Reynolds number is mainly due to heat transfer effects and is negligible. On the other hand, the equivalence ratio and fuel composition have a noticeable effect on flame temperature. In addition, the results show that the landfill gas flames compared to the CH_4 ones have a lower flame temperature. With increment of CO_2 volume fraction at lean combustion, thermal flame height is augmented while at stoichiometric and rich combustion, its value reduced. Thermal flame height augments linearly by Reynolds number increase, while its increment at rich mixture is higher and the effect of Reynolds number at lean mixtures is insignificant. For validation of experimental results from Mach-Zehnder Interferometry, K-type thermocouples are used at peripherally low and moderate isotherm lines.

Key words: *temperature profile, laminar flame, premixed LFG/air, slot burner, Mach-Zehnder interferometer*

Introduction

Due to the diminution of fossil fuel supplies and increment of energy expenditure, the combustion of renewable fuels derived from biomass became gradually important [1]. Landfill gas (LFG) is a kind of biogas, produced by bacterial decomposition, volatilization, and chemical reaction of animal and other type of solid waste [2]. The raw materials can be municipal waste, green waste, plant material, and crops. In the late of 1980s, it was found that LFG is flammable and can be used as a fuel for generating electricity, domestic, and industrial purposes [3].

LFG mostly consists of CH_4 and CO_2 and small amounts of oxygen and nitrogen. The methane volume fraction has a ranging from 50% to 70% that pertains to its formation procedure [4]. Since concentration of carbon dioxide is high, heating value, flame stability, burning velocity and flame temperature are less than other hydrocarbon fuels [5].

* Corresponding author; e-mail: Z_Najafian@ut.ac.ir

Many investigations have been done in order to solve these problems. Lee *et al*. [6] studied the effect of mixing fuels to increase heating value and flame stability of LFG fuel. It was observed that by addition of liquefied petroleum gas (LPG), the heating value and flame stability of mixed fuel was increased, and LFG-LPG can be substituted instead of LFG in domestic combustion appliances. Dai *et al*. [7] investigated the flame stability of premixed biogas flame for reference test burner. Six combustible mixtures were selected and used to study the flame stability in which the CO_2 volume fraction varies in the ranges of 30% to 45%. It was shown that by increasing primary air ratio and CO_2, volume fraction and the lifting limits reduced while the yellow tipping limits enhanced. The effect of hydrogen addition on flame characteristics of biogas in Bunsen burner was studied by Zhen *et al*. [8]. The three biogas composition, BG_{60} (60% CH_4-40% CO_2 on the volume basis), BG_{50} and BG_{40} were chosen and the fraction of hydrogen in the biogas mixtures varies in the range of 10% to 50%. The Reynolds number was selected within the ranges of $400 \leq Re \leq 800$ and equivalence ratio of $0.8 \leq \varphi \leq 1.2$. It was shown that by increments of the hydrogen fractions in fuel mixture, the flame characteristics such as flame stability, laminar burning velocity and flame temperature were augmented. Cardona *et al*. [9] investigated the effects of propane and hydrogen addition on biogas (66% CH_4-34% CO_2) experimentally and numerically. For numerical study, the GRI-Mech 3.0 and C_1-C_3 reaction mechanisms were used. It was shown that by addition of propane and hydrogen, the burning velocity significantly elevated. It was also discerned that for biogas/propane/hydrogen mixture, burning velocity reaches to its maximum at equivalence ratio, $\varphi = 1$, whereas it occurs at $\varphi = 1.1$ for biogas. Liu *et al*. [10] obtained the structure and laminar burning velocity of pyrolysis gases, landfill gases and syngas gases (mixture of CO and H_2) numerically. The flame temperature, burning velocity and species mass fraction of fuel mixtures obtained from the reaction zone. There was a difference between the stoichiometric methane/air flame and LFG_{55}/air flame, and it was discovered that flame temperature and emission of landfill combustion is less than methane combustion.

Landfill gas is reachable in remote rural area and environmentally friendly renewable fuel. The heating value of Landfill gas for domestic combustion appliances and electricity generation satisfies the need. The present work was implemented to study the flame characteristics of LFG_{50} (50% CH_4-50% CO_2) and LFG_{70} (70% CH_4-30% CO_2) fuels and compared with the results of methane/air flame [11] in a slot burner. Temperature value and its distribution depend highly on equivalence ratio and Reynolds number of the unburned combustible mixture. The variation in the equivalence ratio, which leads to a rich and lean mixture, changes the flame temperature and increasing the Reynolds number reforms the structure of the flame. Hence, evaluation of temperature distribution of flame in different states is what we need for a desirable burner design [12]. Equilibrium concentration, emission characteristic and species reaction rate are all related to regional flame temperature [13]. It is essential to obtain the heat transfer rates of combustion processes to investigate the temperature field of the premixed flames [14].

Many experimental methods for temperature measurements have been implemented. Most of the practical techniques are achieved by thermocouple and resistance thermometers [15]. These methods are intrusive, point wise and disturb the temperature field of the region of interest. Optical methods are mainly fast, non-intrusive and accurate [16]. Many optical methods such as Interferometry, Laser speckle technique, Schlieren photography and Moire deflectometry have been examined to observe temperature field of gaseous flames. All the interferometry methods, including Mach-Zehnder interferometry, Talbot interferometry and Holographic interferometry are based on changes in the refractive index of the gaseous products of the flame. By knowing the flame gaseous products and using the Gladstone-Dale relation, the temperature can be calculated [17, 18]. For a premixed flame, the error resulted from diversity in gas composition is less than 2% for equivalence ratio of, $\varphi < 2$ [19, 20]. Therefore, the refractive index of air can be substituted instead of gaseous products of combustion [21].

Laminar premixed LFG flame in a slot burner has rarely been studied. In order to determine the heat transfer rate of combustion processes, it is necessary to obtain temperature field of the premixed flame. Present work is done to obtain temperature profile, thermal flame height and visualize the temperature field of two LFG mixtures (LFG_{50} and LFG_{70}) at different equivalence ratios and Reynolds numbers.

Experimental procedure

Interferometer

Flame structure and temperature field of laminar premixed methane/air combustion is captured using Mach-Zehnder interferometry (MZI) which is a non-intrusive method. A schematic of the interferometer set-up is shown in fig. 1. The interferometer consists of a 10 mW Helium-Neon laser with 632.8 nm wavelength, two doublets, a pinhole, a micro-lens, three flat mirrors (M), two beam splitters (BS) and a CCD camera. The mirror and the Beam Splitters are at parallel position to facilitate the infinite fringe mode. More details about Mach-Zehnder interferometry technique is presented in the literature [22, 23]. All the isotherm patterns are captured by an "ARTCAM-320p" 30 fps CCD camera with 3.2 M pixels, which is connected to a PC to record the images.

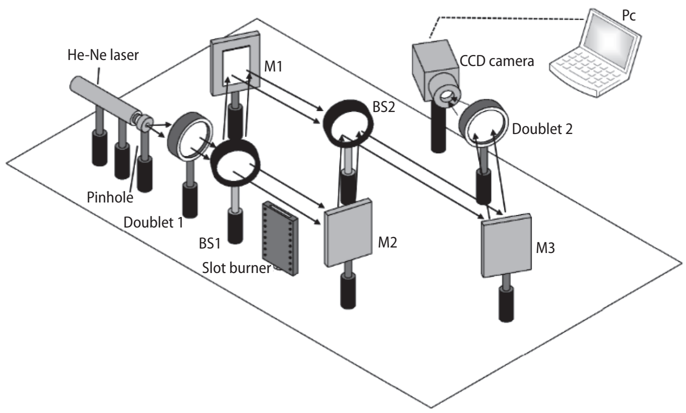

Figure 1. Mach-Zehnder set-up

Experimental set-up

The layout of the experimental set-up is depicted in fig. 2. Flame was generated using a stainless-steel rectangular burner with an inner cross-section of 60 mm × 6 mm and 250 mm height and wall thickness of 3.5 mm. Length to width ratio of the burner is large enough to eliminate three-dimensional effects of flame in z-direction.

In order to obtain a uniform exit velocity profile, the inside surface of the slot burner is highly polished. Furthermore, 1.5 mm diameter stainless-steel balls and a honeycomb section were used at the mixture entrance to the burner in order to prevent non-uniformity of the flow. The geometrical detail of the burner is illustrated in fig. 3. The slot burner is mounted on a positioner which can move both horizontally and vertically to achieve the parallelism of the laser beam with the slot burner length. In order to protect the flame from ambient disturbance, the burner is surrounded by an enclosure with cross-section of 25 cm × 50 cm and height of 150 cm. The enclosure is made up of transparent plexiglas with 5 mm thickness that enables the visualization of the flame structure. Two 10 cm in diameter windows are mounted on the enclosure's walls to let the laser beam pass through the test section.

The CH_4 and CO_2 gases are contained in high pressure cylinders and have over 99.9% purity. The fuels pressure are controlled by two pressure regulating valve. A compressor is used to supply air to the mixer.

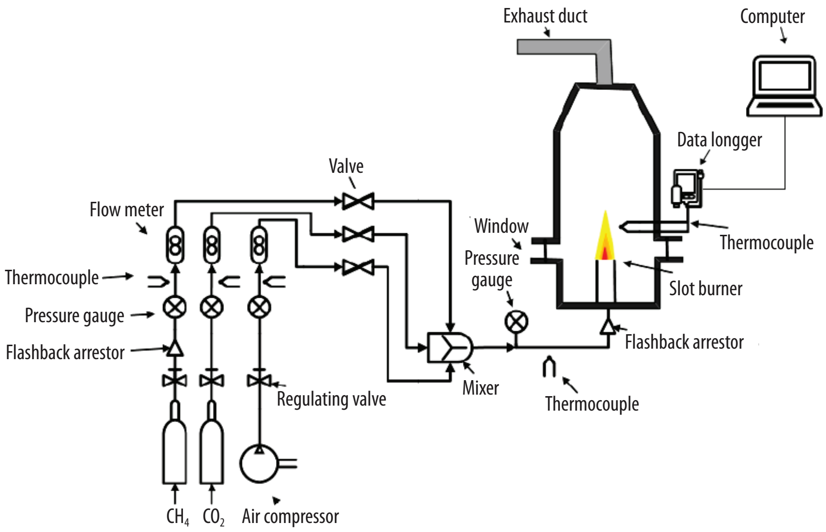

Figure 2. Schematic view of experimental set-up

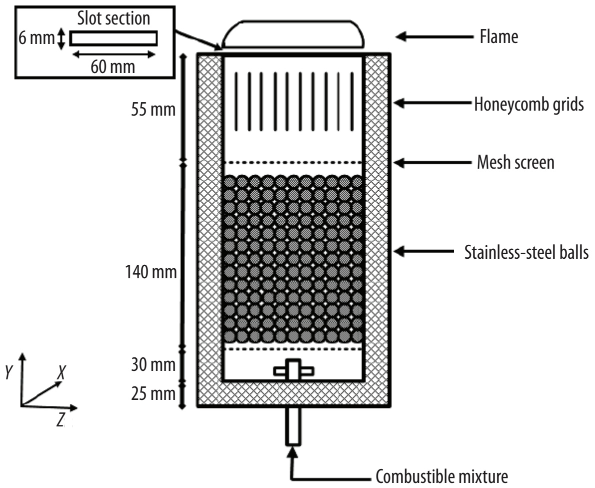

Figure 3. Schematic of the slot burner

The flow rates are measured by three rotameters that each are specifically calibrated for CH_4, CO_2 and air. The calibrated rotameters have an error of 3% of the flow rates at operating conditions. A brass cylindrical mixing chamber filled with stainless-steel balls is utilized to premix the fuel and oxidizer. All the temperatures are recorded using K-type thermocouples and a "TESTO 177" four-channel data logger, which is connected to a PC. All the thermocouples were calibrated in an isothermal bath. In order to prevent the flame flashback in the tube and cylinders, two flashback arrestors are utilized. Further details can be found in fig. 2.

Data reduction

The objective of data reduction procedure in this study is to specify the temperature field of the laminar premixed flame in the slot burner. A code has been developed to obtain the temperature field and isotherm patterns at different Reynolds numbers and equivalence ratios.

When a laser beam crosses through a hot medium, an optical path difference occurs due to the changes of the refractive index in the medium. The optical path difference of two beams separated by the first Beam Splitter (BS1) can be obtained [24] as:

$$\varepsilon = \frac{1}{\lambda_0}\int_0^L \left[n_{\mathrm{ref}} - n(x,y,z) \right] \mathrm{d}z \tag{1}$$

where λ_0 is the wavelength of the laser beam that equals to 638.2 nm, n_{ref} is the refractive index of the air at reference state and $n(x,y,z)$ is the local refractive index of the flame. L is the characteristic length of the burner along the light beam.

In order to obtain reference refractive index the ambient temperature, pressure and relative humidity are required to be measured. As mentioned before, the burner's cross-section dimensions assure two-dimensional assumption and since changes of refractive index in z-direction is negligible. Therefore, eq. (1) is simplified to:

$$\varepsilon = \frac{n_{\rm ref} - n(x,y)}{\lambda_0} L \tag{2}$$

The local refractive index is obtained:

$$n = n_{\rm ref} - \frac{\varepsilon \lambda_0}{L} \tag{3}$$

By determining the local refractive index from eq. (3), Gladstone-Dale equation [25] calculates the local temperature:

$$T(x,y) = \left[\frac{n_{\rm ref} - 1}{n(x.y) - 1} \right] T_{\rm ref} \tag{4}$$

where T_{ref} is the temperature of the undisturbed region near the flame. Equation (4) gives temperature in a specific point of a fringe and since each fringe represents an isotherm, the temperature of the overall fringe is obtained. In this study, twenty photographs were captured to ascertain the reliable fringe patterns at each specific Reynolds number and equivalence ratio. The Reynolds number of slot flame burner was measured corresponding to cold fuel/oxidizer mixture gasses and defined [26]:

$$\mathrm{Re} = \frac{\rho_{\rm mix} V_{\rm exit} D_{\rm h}}{\mu_{\rm mix}} \tag{5}$$

where ρ_{mix} is the density of the gaseous mixture, μ_{mix} – the dynamic viscosity of mixture, D_h – the hydraulic diameter and V_{exit} – the velocity at exit from the slot burner.

The μ_{mix} and D_h are calculated as follows:

$$\mu_{\rm mix} = \frac{\sum\left(\mu_i Y_i \sqrt{M_i}\right)}{\sum\left(Y_i \sqrt{M_i}\right)} \tag{6}$$

$$D_{\rm h} = \frac{4LW}{2(L+W)} \tag{7}$$

where i represents the mixture component, Y_i is the mole fraction, M_i – the molecular weight, L and W are the slot length and width, respectively.

Reliability of experimental results

Uncertainty analysis

The uncertainties of the obtained flame temperature are evaluated from three major sources: the uncertainty of equivalence ratio (φ), uncertainty of Reynolds number and the uncertainty of optical method. The uncertainties in equivalence ratio and Reynolds number are mainly due to uncertainties in the volumetric flow meters of fuel and oxidizer. The uncertainty analysis has been carried out for all the cases. The maximum uncertainties are ±12.7% and ±3.46% for equivalence ratio and Reynolds number, respectively. Detail information about measurement of this uncertainty is presented in [27, 28].

The other source of uncertainty arises from Mach-Zehnder interferometer. Since the refractive index of air is considered as that of the combustion products, it is one of the error sources. The average error for this case is 2.3% at the equivalence ratio of 2 [29] and at the lower equivalence ratio, the error is less than 2% [30].

The second cause for errors in the optical method is changes in the refractive index of air at high temperatures. When the laser beam passes through a premixed slot flame jet, will deviate from its original path. Kharitonov [31] suggested that for temperatures up to 6000 K the variation of air refractive index is negligible and can be considered to that of the air refractive index under normal condition. The last source of error can be due to the constant property assumption for the fuel and air. It was shown that the maximum error for this consideration is less than 3% [32].

Validation

In order to investigate the accuracy of the experimental results and data reduction method, the temperature obtained from the optical method is compared with that of thermocouples at the horizontal line passing through the center of maximum temperature region. The measured flame temperatures with thermocouples were modified to account for the effect of convection and radiation [33]. Figure 4 shows the comparison of the results obtained from the two experimental method at Re = 300 and equivalence ratios of 0.7 and 1 for LFG_{70} and LFG_{50}. Good agreement is obtained between the flame temperature profiles using interferometry compared against the results of thermocouples. Regarding to the thermocouple kind (K type), the validation for higher temperatures than 1400 K was impossible. The maximum discrepancy between the temperature obtained from thermocouples and Mach-Zehnder interferometry technique is 23 °C and 27 °C for the equivalence ratio of 0.7 and 1, respectively.

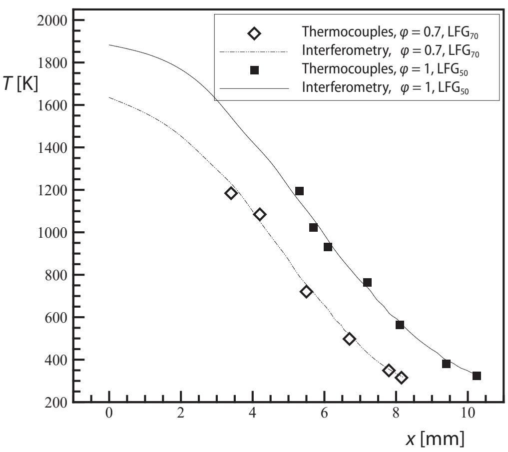

Figure 4. Comparison of the results obtained from MZI and thermocouples

Results and discussion

The effects of Reynolds number and equivalence ratio on the thermal flame height (H_T), flame temperature and structure of LFG flames are studied experimentally with the inlet condition of T_0 = 298 K and P_0 = 0.87 atm. In the present study, the effect of Reynolds number ranging from 100 to 600, which is in the laminar flame region, and equivalence ratios of φ = 0.7, 1 and 1.3 are investigated.

Flame structure

The flame structure of the premixed LFG_{70} fuel at equivalence ratio of, φ = 1.3, Reynolds number of 400 and LFG_{50} fuel at equivalence ratio of unity and Reynolds number of 200 is characterized in fig. 5. According to fig. 5(a), the flame contains three major zones: inner zone of unburned gases, luminous zone of hot radical species and outer zone, which contains mainly complete combustion products. Isotherm lines of corresponding regions in flame zone with their temperature values are presented in fig. 5(b). In this figure, some of the isotherm lines were skipped for clarity. The greatest temperature gradient occurs along the boundary of the inner zone. It is also observed that the maximum temperature occurs just above the inner zone. This vertical distance, from the burner to end of the inner zone, define as thermal flame height (H_T), which indicated in fig. 5(a). Another region of the large temperature gradient is observed at the outer boundary of the flame, where heat is lost rapidly to the low temperature surroundings.

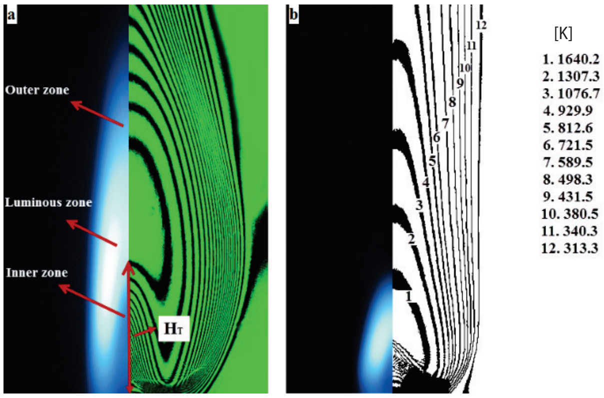

Figure 5. Flame structure and isotherm lines; (a) Re = 400, φ = 1.3, LFG$_{70}$, (b) Re = 200, φ = 1, LFG$_{50}$

Effects of Reynolds number and equivalence ratio

Effect of Reynolds numbers of 400 and 600 at different equivalence ratios of 0.7, 1, and 1.3 on structure of the laminar premixed LFG$_{50}$/air flame is illustrated in fig. 6. As is depicted, by increasing the Reynolds number, the height of the inner zone, which is an indicator of thermal flame height, augments. In fact, the thermal flame height is proportional to Reynolds number. Since Reynolds number is proportional to the inlet average velocity at each equivalence ratio, increasing Reynolds number causes the reaction zone to occur at higher vertical distances.

At lean combustion due to existence of further air, the fuel consumption rate is higher and mixture devours right after escaping from the burner. As air to fuel ratio decreases to the rich values, mixture will need extra air for complete combustion, which leads to flame stretch. Consequently, a longer vertical distance is required for fuel to burn completely, and length of the inner zone will be larger than lean flames. Figure 6 also demonstrates that the effect of Reynolds number on height of the inner zone is more pronounced than the equivalence ratio.

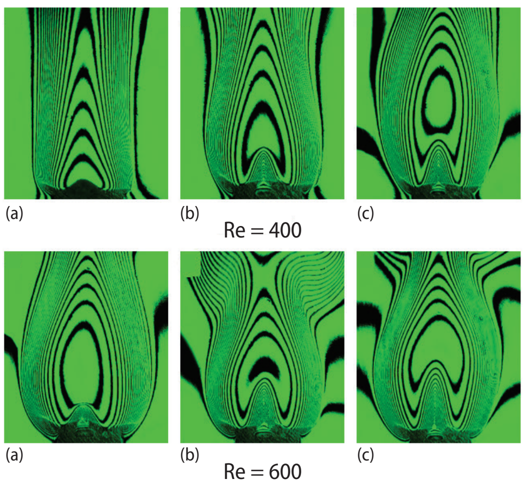

Figure 6. Isotherm lines of the LFG$_{50}$/air at equivalence ratios; (a) φ = 0.7, (b) φ = 1 and (c) φ = 1.3

By shifting from lean to rich mixture, the inner zone of unburned gas stretches and the maximum flame temperature area is enhanced but stability of the flame is decreased. The problem of flame stability is due to air suction by the flame, which causes unwanted cross flow and flame oscillation. Because the structure of the methane and LFG_{70}/air flame is similar to the LFG_{50}/air flame, to avoid repetition, their isotherm patterns are not shown throughout this paper.

Flame temperature

Figure 7 illustrates flame temperature profiles of premixed methane [11], LFG_{70} and LFG_{50}/air flames at Re = 400 and equivalence ratio of unity at a horizontal line which passes through the center of the maximum temperature isotherms. It is observed that at the same level of x, the temperature of methane/air combustion is higher than those of the LFG_{70}/air and LFG_{50}/air flame. This figure reveals a trend that the higher CO_2 concentration in the LFG, the lower the flame temperature. This is because the CO_2 is an inert gas. The presence of CO_2 in the LFG dilutes the hot combustion gases during the burning process of the fuel, and these diluents would simply absorb heat from the combustion process. In addition, the CO_2 gas is a good radiation emitter, and thus the radiation energy loss tends to be larger in the flame diluted by CO_2, further contributing to its lower temperature. The maximum temperature of stoichiometric of methane flame is 2011 K, which is 0.91 of adiabatic flame temperature. The difference is mainly due to heat transfer effects and air suction from the periphery medium. This figure also points out that the maximum temperatures of LFG_{70} and LFG_{50} are 1949 K and 1889 K, respectively. Although the LFG fuel includes about 30% and 50% of inert gas such as CO_2 for LFG_{70} and LFG_{50}, the flame temperature get relatively as high as 1850 K at stoichiometric condition.

Figure 8 shows the distribution of temperature in the reaction zone for the lean and rich LFG flames. The temperature profile of LFG_{50} flame also show a similar trend to that of the LFG_{70} flame excepting that the maximum temperature value of LFG_{70} is slightly higher than LFG_{50}. At lean combustion, $\varphi = 0.7$, in the same level of x, the flame temperature of LFG_{50} is higher than LFG_{70} while maximum flame temperature of LFG_{70} is 50 K higher than LFG_{50}. At rich condition, $\varphi = 1.3$, temperature of LFG_{70} is almost higher than LFG_{50} in all horizontal locations.

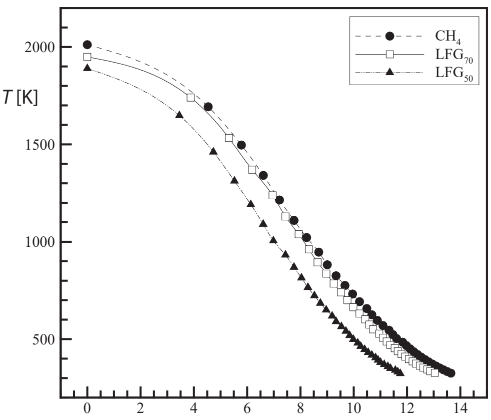

Figure 7. Flame Temperature profile for methane, LFG_{70}, LFG_{50} at $\varphi = 1$ and Re = 400

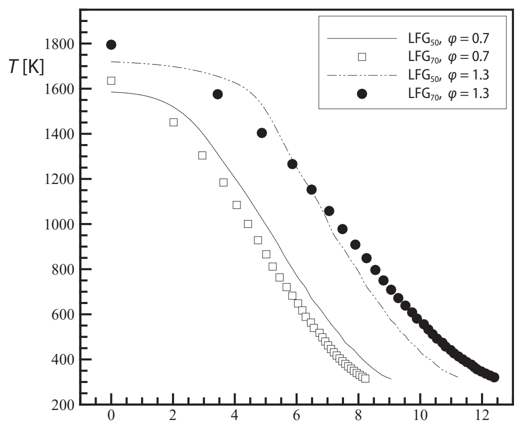

Figure 8. Temperature profile of LFG_{50} and LFG_{70} at $\varphi = 0.7$, 1.3 at Re = 300

Maximum flame temperature of methane, LFG_{70} and LFG_{50} at different equivalence ratio ranging from 0.7 to 1.3 is shown in fig. 9. The figure shows that the flame with $\varphi = 1$ has the highest temperature among all the flames within $0.7 \le \varphi \le 1.3$. It is simply because relatively more complete combustion occurs at $\varphi = 1$ than other equivalence ratios. As the flame becomes richer, incomplete combustion occurs and results in monotonically lower temperature at higher equivalence ratios. At lean combustion, due to further air, the fuel consumption rate is high and the extra air which does not participate in the combustion processes causes to lower flame temperature. The figure also shows that the methane flame has a higher temperature than the LFG fuels due to the lower LHV in the LFG gas flame.

In fig. 10 the maximum flame temperature obtaining from data reduction is shown at different Reynolds numbers and equivalence ratios. Although by increasing the Reynolds number, heat flux is enhanced, but the maximum flame temperature change is negligible. At the constant equivalence ratio of unity, by increasing Reynolds number from Re = 100 to 600, the maximum temperature difference of 35 K is observed.

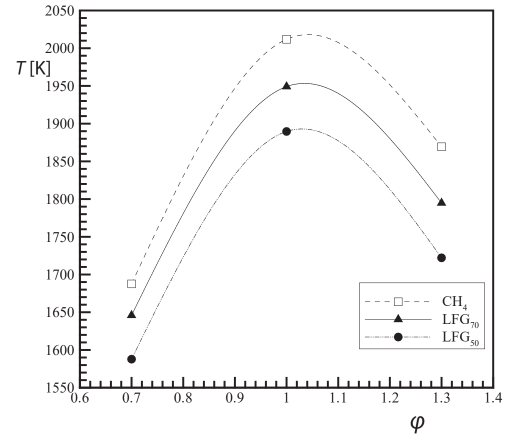

Figure 9. Maximum temperature of methane, LFG_{70} and LFG_{50} at different equivalence ratios and Re = 400

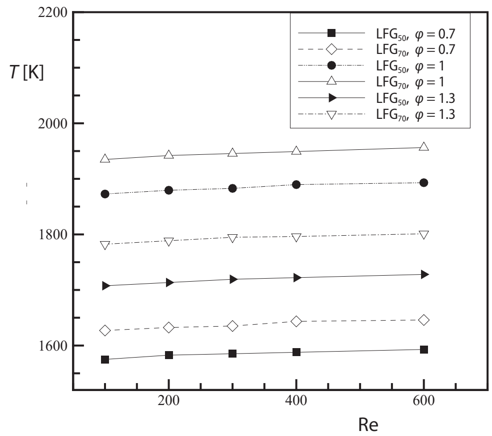

Figure 10. Maximum flame temperature at different equivalence ratios and Re numbers

Flame temperature of LFG_{50} fuel along the horizontal line passing through the maximum temperature point at different Reynolds number at stoichiometric condition are shown in fig. 11. By increasing Reynolds number flame expands and a greater area is affected by heat flux from combustion zone. These results show that LFG has a sufficient potential as alternative fuel with respect to flame temperature and may be utilized usefully in various types of combustion equipment.

Thermal flame height

The thermal flame height is considered as an important parameter in characterizing the structure of premixed flames. Thermal flame height (H_T) defined as the vertical distance from the burner at which the temperature is maximized [34], occurs just above the inner zone [35].

Thermal flame height for Reynolds number ranging from 100 to 600 and equivalence ratio of 0.7 is illustrated in fig. 12. It is observed that the thermal flame height enhanced almost linearly with increment of Reynolds number up to 400, and after that, its increment becomes insignificant. The change in thermal flame height is around 76.19%, 98.66%, and 118.9% for CH_4, LFG_{70} and LFG_{50}, respectively. By increasing CO_2, thermal flame height is augmented at lean combustion.

Thermal flame height at equivalence ratios of, $\varphi = 1$ and $\varphi = 1.3$ are shown in figs. 13(a) and (b), respectively. The changes in thermal flame height is about 371.78%, 285.36%, and 280.36% at $\varphi = 1$ and 326.12%, 323.31% and 307.13% at $\varphi = 1.3$ for CH_4, LFG_{70}, and LFG_{50}, respectively. Despite the lean combustion, at stoichiometric and rich combustion, by increasing the CO_2 thermal flame height reduced. The thermal flame heights of LFG fuels also

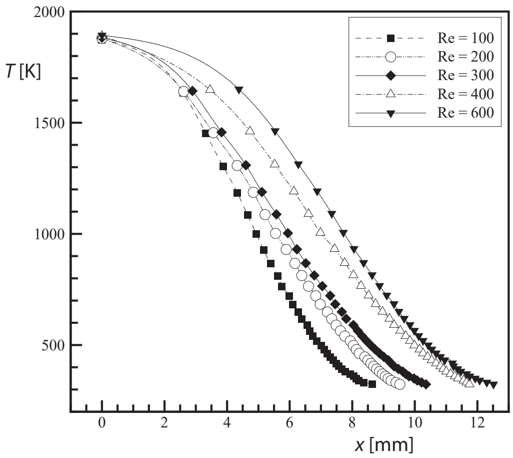

Figure 11. Temperature profile at equivalence ratio of unity and different Re numbers for LFG_{50}

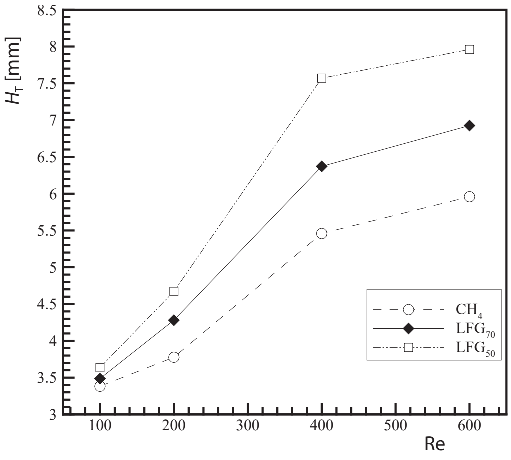

Figure 12. Thermal flame height at different Re numbers and φ = 0.7

show a similar trend to that of CH_4, and their relationships are linearly with Reynolds number increment. As shown in figs. 12 and 13, by increasing equivalence ratio from $\varphi = 0.7$ to $\varphi = 1.3$, the thermal flame height is increased and the tip of the flame cone moves upward. Therefore, the effect of an increase in the equivalence ratio is to reduce the maximum flame temperature and meantime move the location of the maximum temperature region upward.

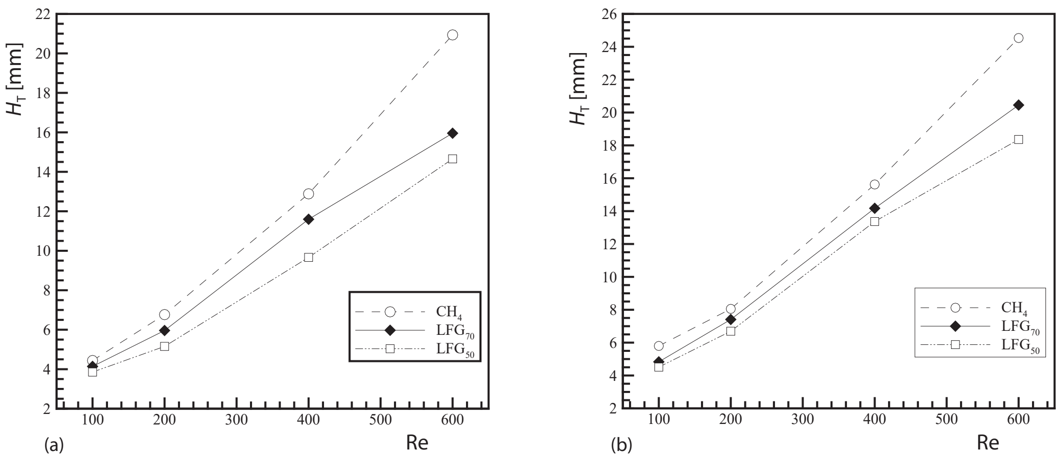

Figure 13. Thermal flame height at different Reynolds numbers; (a) φ = 1, (b) φ = 1.3

Conclusions

The Mach-Zehnder interferometry technique as an accurate and nonintrusive method is utilized to measure and visualize the two-dimensional laminar LFG flames. Good agreement is observed between optical method and thermocouples results, which show its ability to be used instead of other experimental methods. Three major regions are observed in flame, which clearly characterizes its structure, flame height and reaction zone. The effects of Reynolds number ranging from 100 to 600 and equivalence ratio ranging from 0.7 to 1.3 on isotherm lines and temperature profiles are studied experimentally and the results of the present investigation are summarized as follows.

- The results show that by increasing Reynolds number, the height of the inner zone is augmented and the peak of the flame temperature occurs at a higher vertical distance. In addition, by increments of Reynolds number flame expands and a greater area is heated, but variation in maximum gas temperature is negligible.
- The effect of gas composition on thermal flame height (H_T), structure, temperature profile and isotherm lines is studied experimentally. By increasing inert gas such as CO_2, the flame temperature and thermal flame height at rich combustion are reduced; while at lean combustion, thermal flame height is augmented. In addition, the results indicate that the thermal flame height enhanced almost linearly with increment of Reynolds number at each equivalence ratio.
- The effect of Reynolds number on thermal flame height at stoichiometric and rich combustion is more pronounced than the lean combustion. By increasing or decreasing equivalence ratio due to incomplete combustion, the flame temperature and its stability are reduced.

References

[1] Zhen, H., *et al*., Effects of Hydrogen Addition on the Characteristics of a Biogas Diffusion Flame, *International Journal of Hydrogen Energy*, *38* (2013), 16, pp. 6874-6881
[2] Lee, C.-E., *et al*., A Study on the Determination of Burning Velocities of LFG and LFG-Mixed Fuels, *Fuel*, *81* (2002), 13, pp. 1679-1686
[3] Porteous, A., Developments in, and Environmental Impacts of, Electricity Generation From Municipal Solid Waste and Landfill Gas Combustion, *IEE Science, Measurement and Technology*, *140* (1993) 1, pp. 86-93
[4] Zhen, H., *et al*., A Comparison of the Heat Transfer Behaviors of Biogas–H2 Diffusion and Premixed Flames, *International Journal of Hydrogen Energy*, *39* (2014), 2, pp. 1137-1144
[5] Li, X., *et al*., Study on Stretch Extinction Limits of CH_4/CO_2 versus High Temperature O_2/CO_2 Counterflow Non-Premixed Flames, *Combustion and Flame*, *161* (2014), 6, pp. 1526-1536
[6] Lee, C.-E., *et al*., A Study on the Interchangeability of LFG–LPG Mixed Fuels with LFG Quality in Domestic Combustion Appliances, *Fuel*, *87* (2008), 3, pp. 297-303
[7] Dai, W., *et al*., Experimental Studies of Flame Stability Limits of Biogas Flame, *Energy Conversion and Management*, *63* (2012), Nov., pp. 157-161
[8] Zhen, H., *et al*., Characterization of Biogas-Hydrogen Premixed Flames Using Bunsen Burner, *International Journal of Hydrogen Energy*, *39* (2014), 25, pp. 13292-13299
[9] Cardona, C. A., Amell, A. A., Laminar Burning Velocity and Interchangeability Analysis of Biogas/C_3H_8/H_2 with Normal and Oxygen-Enriched Air, *International Journal of Hydrogen Energy*, *38* (2013), 19, pp. 7994-8001
[10] Liu, C., *et al*., Structures and Burning Velocity of Biomass Derived Gas Flames, *International Journal of Hydrogen Energy*, *35* (2010), 2, pp. 542-555
[11] Ashrafi, Z. N., *et al*., Two-Dimensional Temperature Field Measurement of a Premixed Methane/Air Flame Using Mach-Zehnder Interferometry, *Optics Communications*, *341* (2015), Apr., pp. 55-63
[12] Glassman, I., *Combustion*, Academic Press, New York, USA, 1997
[13] Ahmadi, M., *et al*., Temperature Measurement of a Premixed Radially Symmetric Methane Flame Jet Using the Mach-Zehnder Interferometry, *Optics and Lasers in Engineering*, *49* (2011), 7, pp. 859-865
[14] Remie, M., *et al*., Heat-Transfer Distribution for an Impinging Laminar Flame Jet to a Flat Plate, *International Journal of Heat and Mass Transfer*, *51* (2008), 11-12, pp. 3144-3152
[15] Fujisawa, N., Flickering Characteristics and Temperature Field of Premixed Methane/Air Flame Under the Influence of Co-Flow, *Energy Conversion and Management*, *78* (2014), Feb., pp. 374-385
[16] Hariharan, P., *Optical Interferometry*, Academic Press, New York, USA, 2003
[17] Gladstone, J. H., Dale, T., Researches on the Refraction, Dispersion, and Sensitiveness of Liquids, *Philosophical Transactions of the Royal Society of London*, *153* (1863), Mar., pp. 317-343
[18] Francesconi, R., Ottani, S., Correlation of Density and Refraction Index for Liquid Binary Mixtures Containing Polyglycols. Use of the Group Contributions in the Lorentz–Lorenz, Gladstone–Dale and

Vogel Equations to Evaluate the Density of Mixtures, *Journal of Molecular Liquids*, *133* (2007), 1-3, pp. 125-133
[19] Van Der Wege, B. A., *et al*., Quantitative Shearography in Axisymmetric Gas Temperature Measurements, *Optics and Lasers in Engineering*, *31* (1999), 1, pp. 21-39
[20] Stella, A., *et al*., Measurement of Axisymmetric Temperature Fields Using Reference Beam and Shearing Interferometry for Application to Flames, *Experiments in Fluids*, *29* (2000), 1, pp. 1-12
[21] Qi, J., *et al*., Temperature-Field Measurements of a Premixed Butane/Air Circular Impinging-Flame Using Reference-Beam Interferometry, *Applied Energy*, *83* (2006), 12, pp. 1307-1316
[22] Hauf, W., Grigull, U., Optical Methods in Heat Transfer, *Advances in Heat Transfer*, *6* (1970), pp. 133-366
[23] Flack Jr, R. D., Mach-Zehnder Interferometer Errors Resulting from Test Section Misalignment, *Applied Optics*, *17* (1978), pp. 985-987
[24] Eckert, E. R., Goldstein, R. J., *Measurements in Heat Transfer*, Taylor & Francis, Oxford, UK, 1976
[25] Qi, J., *et al*., Temperature Field Measurement of a Premixed Butane/Air Slot Laminar Flame Jet with Mach–Zehnder Interferometry, *Applied Thermal Engineering*, *28* (2008), 14-15, pp. 1806-1812
[26] Dong, L., *et al*., Heat Transfer from an Impinging Premixed Butane/Air Slot Flame Jet, *International Journal of Heat and Mass Transfer*, *45* (2002), 5, pp. 979-992
[27] Holman, J., *Experimental Methods for Engineers*, McGraw and Hill Inc., New York, USA, 1994
[28] Bosschaart, K. J., De Goey, L., Detailed Analysis of the Heat Flux Method for Measuring Burning Velocities, *Combustion and Flame*, *132* (2003), 1-2, pp. 170-180
[29] Qin, X., *et al*., Effect of Varying Composition on Temperature Reconstructions Obtained from Refractive Index Measurements in Flames, *Combustion and Flame*, *128* (2002), 1-2, pp. 121-132
[30] Chen, C.-C., *et al*., Effect of Composition Change on Temperature Measurements in a Premixed Flame by Holographic Interferometry, *Optical Engineering*, *31* (1992), 2, pp. 353-362
[31] Kharitonov, A., *et al*., Temperature Dependence of Air Refraction at High Temperatures, *Fluid Dynamics*, *9* (1974), 5, pp. 851-853
[32] Reuss, D. L., Temperature Measurements in a Radially Symmetric Flame Using Holographic Interferometry, *Combustion and Flame*, *49* (1983), 1-3, pp. 207-219
[33] Bradley, D., Matthews, K., Measurement of High Gas Temperatures with Fine Wire Thermocouples, *Journal of Mechanical Engineering Science*, *10* (1968), 4, pp. 299-305
[34] Bennett, B. A. V., *et al*., Computational and Experimental Study of Axisymmetric Coflow Partially Premixed Methane/Air Flames, *Combustion and Flame*, *123* (2000), 4, pp. 522-546
[35] Xiao, X., *et al*., Temperature Measurements in Steady Two-Dimensional Partially Premixed Flames Using Laser Interferometric Holography, *Combustion and Flame*, *120* (2000), 3, pp. 318-332

Paper submitted: November 13, 2014
Paper revised: November 20, 2014
Paper accepted: December 21, 2014